Optical Engineering

SPIEDigitalLibrary.org/oe

Interferogram smoothing and skelotonizing using Bessel functions of the first kind

Dayana H. Penalver
David L. Romero-Antequera
Fermín-Salomón Granados-Agustín

SPIE

Interferogram smoothing and skelotonizing using Bessel functions of the first kind

Dayana H. Penalver
David L. Romero-Antequera
Fermín-Salomón Granados-Agustín
Instituto Nacional de Astrofísica
Optica y Electrónica
Calle Luis Enrique Erro No. 1. Tonantzintla
Puebla, C.P. 72000, México
E-mail: dromero.fisica@gmail.com

Abstract. A new approach for smoothing and fringe normalization is proposed, using Bessel functions of the first kind to fit the intensity distribution, with application for skeletonizing and cancel background illumination in an interferogram. With this approach, high-frequency noise is immunized, and the contrast is enhanced by the computation of fitting coefficients by means of least squares. The new smoothing process works very well also with asymmetric interferograms. Its main advantages are the simplicity of implementation and almost automatic fringe skeletonizing and overcoming the problem of the nonuniformity illumination. © *2012 Society of Photo-Optical Instrumentation Engineers (SPIE).* [DOI: 10.1117/1.OE.51.4.045601]

Subject terms: image enhancement; image segmentation; interferometry.

Paper 111311 received Oct. 20, 2011; revised manuscript received Feb. 21, 2012; accepted for publication Feb. 22, 2012; published online Apr. 11, 2012.

1 Introduction

The analysis of interferogram, band tracking, and skeletonizing is a long studied problem.[1] Automatic analysis exhibits applications that range from the classical, such as skeletonizing of holographic interferograms,[2] profilometric measures,[3] topographic maps,[4] and up to the newest applications such as SAR interferometric analysis.[5] As a long studied problem, nowadays there are many different techniques that involve analysis using Fourier transforms,[6] Zernike polynomial data fitting,[7] and gradient filters.[1] In every other case, a preprocessing of the image is a must in order to improve fringe visibility and regularization for a better processing.

When using Fourier transform techniques, it is required to remove signals of frequencies apart from those the analyst consider to be the characteristic frequencies of the problem (high frequencies usually represent noise, and low frequencies usually represent nonuniform illumination). Even when this process is clear enough and straightforward, it requires the criteria of an operator to perform correctly. Of course, it also has some limitations, as it is difficult to filter spurious frequencies when those are similar to the characteristic ones, and the process is even more complicated whenever there are low-contrast fringes. This stage is usually addressed as spatial filtering.[1]

Another approach to spatial filtering is based in combination of techniques for image-quality improvement, as the one presented, for example, by Chuen-Lin et al.[7] They developed an algorithm based on the Zernike polynomial fitting to eliminate background illumination. Then they segmented the image in positive and negative regions and determined the local maximun and minimun and finally applied a local region contrast modulation to modulate the amplitude of the fringes. Chuen-Lin et al. suggest the applicability of this method for the extraction of the phase.

Another commonly used technique is the fringe skeletonizing, which involves search of local irradiance peaks by many different methods, including local fitting around the peak.[1,8] Although the skeletonizing is less commonly used these days, it has the advantage of quickly presenting basic information such as surface shapes and deviations. Even now, some optical shops use this method for preliminary inspection of the elements under fabrication.

All of these procedures can be used in general situations given the flexibility for which they were intended. However, in the case of analysis of interferograms, the situation is always the same: a fringe pattern. It is our proposal that the spatial filtering (and skeletonizing) can be performed in a simpler way if the inherent oscillating pattern is taken into account.

We present here a smoothing process for the fringes in an interferogram based in a linear least squares fitting with Bessel functions of the first kind, who serves two purposes simultaneously: mitigate the effect of different types of noise on digitized images (particularly multiplicative noise), and being a support framework to easily perform interferogram skeletonizing. Another important potential application is the reduction of background illumination bias, which is briefly discussed here, and the details are being published elsewhere.

In the next section, the regularization process is presented, with some emphasis on computer implementation. Then fringe skeletonizing is presented based on the results of the regularization process and the background suppression is discussed. Finally we draw some conclusions.

2 Image Smoothing by Means of Fitting Using Bessel Functions

We propose a new smoothing process using the Bessel functions of the first kind $J_n(x)$ to fit the intensity distribution of the rows or columns of the image of interferograms. The resemblance between the Bessel functions and the resulting interference pattern along one direction makes this a suitable method to smooth the intensity functions and thus reduce the noise due to experimental features. It is interesting to note how similar are the Bessel J_0 function and the $\sin(x)/x$ function, which is the propagated field in the Fraunhoffer approximation from a single slit.

The kind of smoothing we apropose here is similar to the Savitzky-Golay filter,[9] which is based in a polynomial

fitting. This filter is characterized by simplicity and speed. Our proposal here preserves the same characteristics.

Consider an interference pattern with straight fringes, which has the lateral shearing in the horizontal direction. The digitized image of the interferogram is a matrix whose elements represent the average of the intensity over the sampling points expressed in some arbitrary scale ([0,1] in our case). If the number of sampling points is high enough (which is usually the case), we can regard an array of the image (rows or columns) as a very good discrete approximation of the continuum distribution of intensity. For the sake of clarity, we will refer to such an array as a *slice* of the interferogram. The smoothing process is carried out as follows:

1. Select an slice of the interferogram (row if the shearing is in the horizontal direction and column if the shearing is in the vertical direction).
2. Compute the fitting coefficients by means of least squares, using the following model:

$$f(q) \cong \sum_{k=0}^{N} a_k J_k(\alpha q), \tag{1}$$

   where q is the coordinate in the slice, α is a control parameter of the oscillation (usually $k = 1$) This coordinate has to span within a compact support with the same number of sampling points as those within the slice. However, it is clear that the limits of the support $[a, b]$ are arbitrary. With basis on the experience, we found good results with the intervals [0, 100] and $[-100, 100]$. It is very important to include 0 in the interval.
3. Reconstruct the slice using the approximation given by Eq. (1).
4. Move to the next slice.

The coefficients in the expansion are computed as follows: let $\mathbf{M}$ be the matrix whose entries are: $m_{ik} = J_k(kq_i)$, where J_k is the k'th Bessel function ($k = 0, \cdots, N-1$) and q_i is the coordinate of the i'th pixel along the current slice. Then the N coefficients are computed from the following relation:

$$\mathbf{M}\vec{\mathbf{A}} = \vec{\mathbf{F}}, \tag{2}$$

where $\vec{\mathbf{A}}$ is a column vector whose entries are the coefficients a_k, and $\tilde{\mathbf{F}}$ is a column vector with the values of intensity of the interferogram $f(q_i)$. When dealing with rectangular interferograms, the number of pixels per slice is held fixed, and one can choose N to match accordingly. However, in the general situation, the number of functions and the number of pixels could not match; for example: when smoothing interferograms in circular domains (like the ones considered here), the number of pixels per slice changes and if N is fixed, the system would be underdetermined or overdetermined depending on the slice under consideration. The usual way to proceed is to compute the Moore-Penrose generalized inverse,[10] which computes a good approximation for the coefficients in the least-square sense. A flow chart of the process can be seen on Fig. 1.

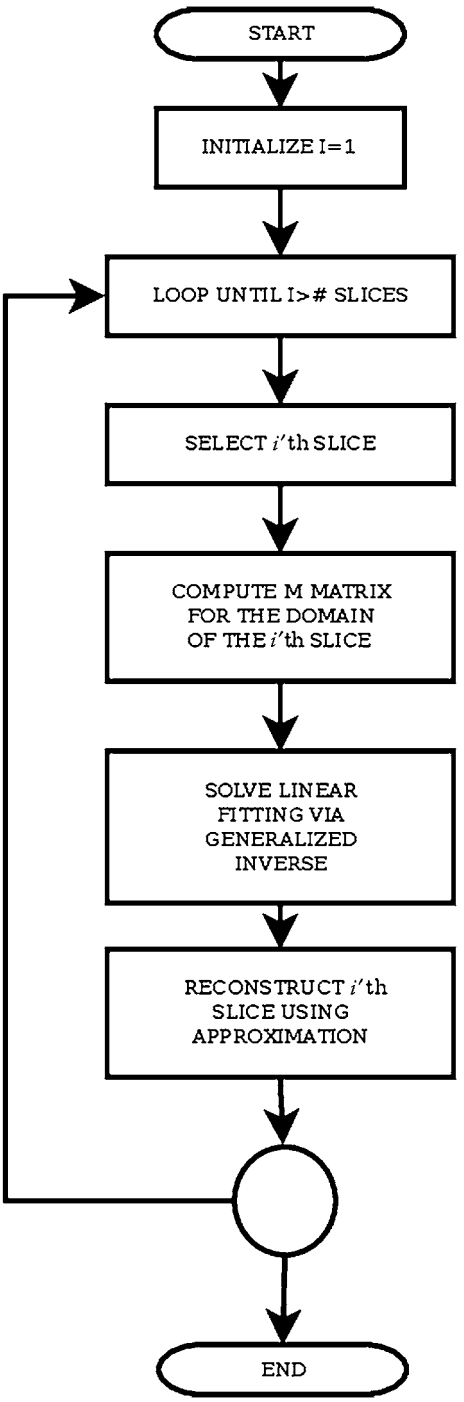

Fig. 1 Flow chart of the smoothing process.

It is important to notice that there is no need to address orthogonality of the functions on Eq. (1), even if dealing with a discrete domain. The model is appropriate for our purposes because the approximation is unable to represent high spatial frequency noise or, as we shall show below, multiplicative noise. One of the key points to perform the fitting is an appropriate number of functions for the profile reconstruction. With basis on the experience, around $N = 100$ would work for most interferograms. Even if this is a relatively high number of functions needed to the fitting (compared to, for example, Zernike polynomials), commodity laptop computers can execute such a process in a picture

of 400×400 pixels in less than a tenth of a second using, for example, MATLAB.

Figure 2 shows examples of typical slices taken from lateral shearing interferograms. The dots and segmented lines represent the intensity values of the original images, and the solid lines is the intensity reconstructed with Bessel functions. Figure 2(a) shows a slice of a interference pattern almost noiseless, Fig. 2(b) shows a slice with mild noise, and Fig. 2(c) exhibits a noisy slice. It is clear from the pictures that the reconstruction is carried out successfully at least for each slice in the direction of the shearing, having a considerable number of functions.

The overall effect of the smoothing process acting over the entire interferogram is depicted in Fig. 3. A set of few intensity slices are bundled and displayed below each interferogram for a better appreciation of the effect of the smoothing process. It can be seen how the smoothing blurs the interferogram horizontally, and comparing the intensity surfaces, one can observe how the noise is reduced after the process. It is also interesting to note that irregular background illumination is enhanced with the smoothing process.

If the number of functions is not high enough, the reconstruction only performs on a vicinity of 0 in the q coordinate system, [Fig. 4(b)]. Additionally, a strong aliasing-like effect takes place for the reconstructed region. This occurs because the first lobe of the Bessel function, in the $-q$ or $+q$ directions, contributes the most to the fitting process. In some sense, each function provides a displaced lobe with respect to the origin that can be used to fit the closest fringe to it. This process is somewhat similar to the use of Gaussian functions

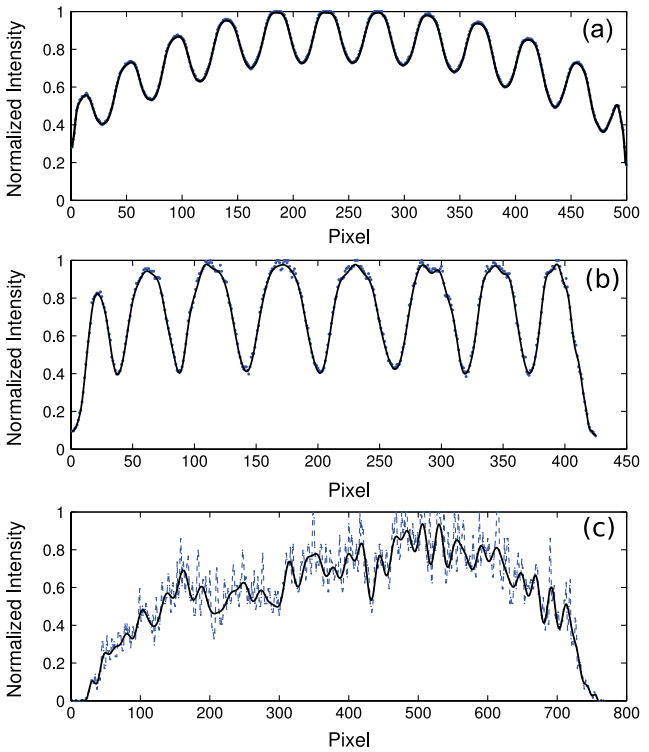

Fig. 2 Intensity profile of different interferometric patterns. (a) A slice of an interference pattern almost noiseless; (b) slice with mild noise; and (c) a very noisy slice. The dots lines in (a) and (b), and the segmented line in (c), represent the intensity values of the original images. The solid lines in all the figures are the intensity reconstructed with Bessel functions.

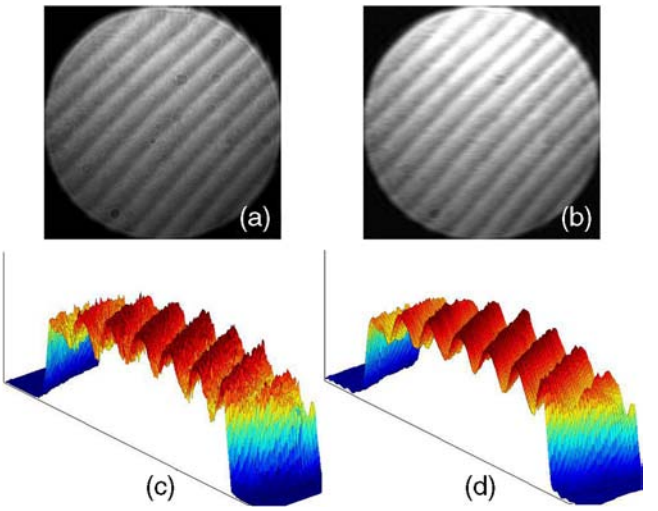

Fig. 3 The overall effect of the smoothing process acting over an interferometric pattern. (a) A interferometric pattern with mild noise; (b) the interferometric pattern of the figure (a) reconstructed with the Bessel functions; (c) and (d) are the distribution intensity function of a segment of the interferometric pattern of the figure (a) and (b), respectively.

in the neighborhood of fringe maxima in order to estimate the locus of the interference fringes, but having the advantage of being easier to implement and performing almost automatically over the slice.

The process can be effectively used to improve contaminated interferograms. In a general case, for interferograms with curved fringes, the best result is achieved executing the process both horizontally and vertically, and then taking the average of both images. This can be seen in Fig. 4(a). We show quantitatively in the Appendix that the process reduces the effect of different types of noises on the image, even for complicated noises such as multiplicative noise; we also perform a comparison between our regularization process and the adaptive Wiener filter.[11] If there is interest on performing fringe detection (skeletonizing), it is a better idea to perform the smoothing separately in both directions and executing maxima detection, as is explained in the next section.

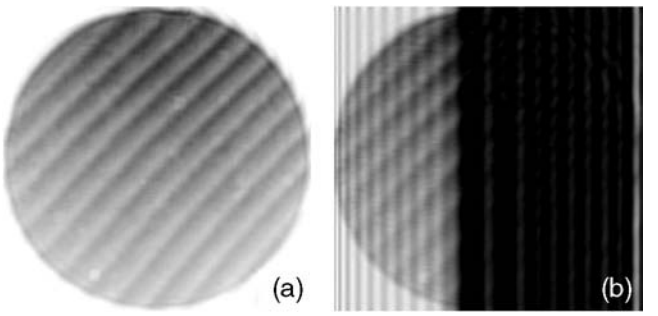

Fig. 4 (a) The interferometric pattern reconstructed using 120 Bessel functions. The process was applied in both directions, horizontally and vertically. (b) Reconstruction of the interferometric pattern using 30 Bessel functions in the horizontal direction, the wave subpatterns arises at the reconstruction region.

3 Skeletonizing Interferograms

The process of skeletonizing interferograms is part of fringe analysis. The skeletonizing is the search of loci of maximum intensity of the interferometric pattern. Different methods are used to achieve that goal, i.e. adaptive thresholds, gradient operators, piecewise approximations, thinning procedures, or spatial frequency filtering. In our case, we used a peak detection algorithm based on image dilation by means of a plain structural Strel element.[12] This simple code that allowed us to test the potentials of the method proposed in the Sec. 2.

In all of these methods the noise of the images plays a crucial role in the detection of maximum of the fringes, in the sense that it degrades the image, difficulting the task. Preprocessing of images using the Bessel smoothing process, improves maxima detection. This can be seen, for example, in Fig. 5; it is difficult to select a pixel from the original image as maximum, but once the smoothing process has been applied, it can be done unambiguously. It is worth nothing that the pixel with the highest value could, in some cases (as the one shown), not match with the actual maximum of the fitted function. However, in these cases it is impossible to distinguish the real maximum from noise deviations; the method allows to specify a maximum based on the smoothness of the function.

The skeletonizing process depends on the fringes inclination, for the case of straight lines the skeletonizing is applied just in the direction of the displacement, but in the case of curved fringes the method must be applied in both directions, i.e. horizontally and vertically. The resulting image is the overlapping of the individual skeletons in each direction. The skeletonizing process is carried out as follows:

1. Apply the Bessel smoothing process to the interferometric image. The use of Bessel filter allows a correct maxima and/or minimums detection.
2. Find the loci of the maximum of the lobes in the horizontal and vertical direction.
3. Using a thresholding process on both images. Then the images are binarized, i.e., the pixels values less than 0.5 are taken to zero and only those that have values over 0.5 are set to one.
4. The resulting binarized images are combined using an "OR" operation.

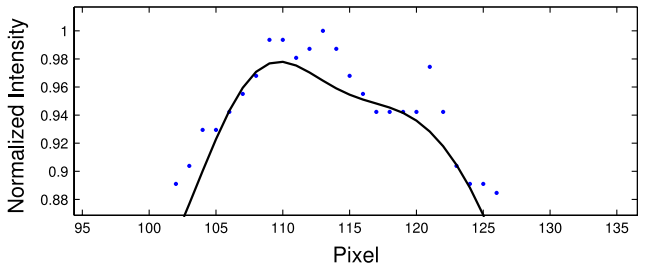

Fig. 5 Smoothed intensity distribution in the vicinity of a fringe maxima. The dotted points represent the values of intensity in the original image, and the continuous line is the least square fitting using 120 Bessel functions. To improve the fitting, a larger number of function are required. For our purposes, this number of Bessel functions is good enough since we want to reduce the marginal noise.

Figure 6 shows interferograms with vortex-like features[13] an the resulting skeletonizing. Since the fringes are curved, the maximum detection is possible by combining the two skeletons. Individually, each skeletonizing does not comprise all of the features of the fringe pattern, having troubles on the detection of loci in the direction orthogonal to the scanning. It must be noticed that this adds some noise to the final skeleton that must be filtered somehow (for example, another filter can be used prior to the smoothing process). The noise is also induced by the presence of aliasing in the images, which can be controlled by changing the resolution of the image under consideration (i.e., changing the sampling rate). However, in most cases, this does not interfere with the band tracking. We performed band tracking once the skeleton was computed using track of pixel connections using eight-connected neighborhoods.

It is important here to clarify something: skeletonizing is different to band-tracking. In the band tracking process, we can identify a set of coordinates (maxima) with an specifically numbered band, while skeletonizing is just the detection of the maxima over the image. It is easy to accomplish band tracking with computer assistance using digital topological algorithms[14] when the skeletonizing has been already performed. The specific problems dealing with broken skeleton lines and numbering have to be dealt from the band-tracking point of view; if using, for example, neighborhood tracking, the lines with separations greater than two pixels will not be connected. In order to solve such a situation, an additional technique must be employed, such as interpolation.

The skeletons can be used to compute "upper" and "lower" envelopes. The skeleton correspond to the loci of

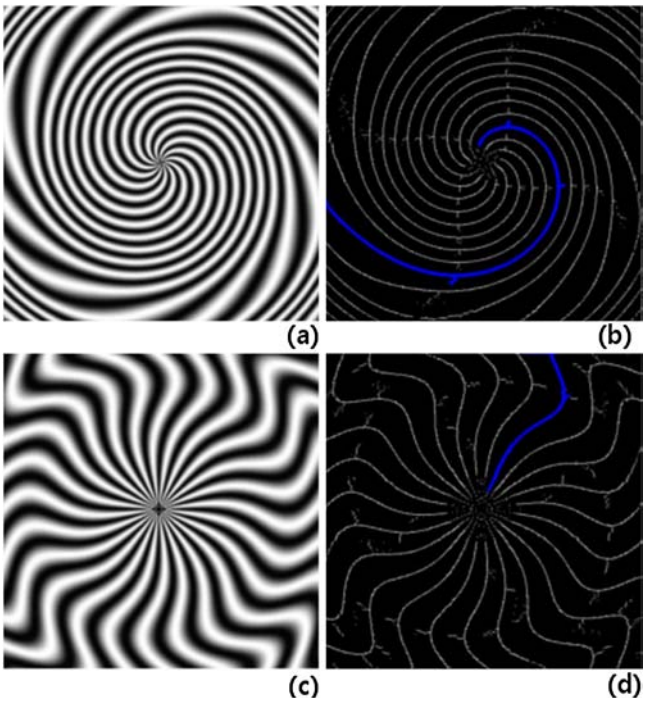

Fig. 6 Skeletonized interferometric pattern with vortices. (a) Is the interference of a wave with radial phase variation and a reference wave with phase $\phi_{r1} = m\theta$. (b) Is the interference of a reference wave $\phi_{r2} = m\theta + Cr$ with a wave with radial phase variation. (c) and (d) are their respective skeletonized images. The blue line is the selection of one of the bands. The interferograms were taken from Ref. 13.

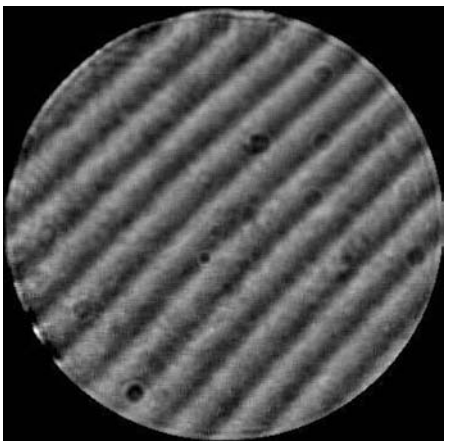

Fig. 7 Interferogram of Fig. 3 with suppression of background illumination and smoothed by means of the Bessel regularization process.

maxima of the image, which is a mask that can be used to sample the maximum values of the intensity of the interferogram. If the image is inverted, the loci of minimums can be computed and thus obtain a mask for sampling minimums values of the intensity of the interferogram. Choosing an appropriate basis (for example, Zernike polynomials), an expansion of the envelopes can be computed via least squares. This information can be used to compute the local fringe visibility:

$$\nu(x,y) = \frac{E_u(x,y) - E_l(x,y)}{E_u(x,y) + E_l(x,y)}, \tag{3}$$

where E_u and E_l are the upper and lower envelopes. The background illumination can be computed as the average of the envelopes. Using these two quantities, it is possible to correct the interferogram using the intensity as proposed, for example, by Schemm and Vest.[15] As an example, we can see the corrected interferogram of Fig. 3 on Fig. 7. The details of the process are being published elsewhere.

4 Conclusions

The regularization process can diminish effects of noise because the Bessel functions are unable to fit to very high-frequency signals, thus eliminating those on the reconstruction of the image, just like the Savitzky-Golay filter.[9] Also, tests have shown the algorithm robust enough to deal with nonuniform illumination. On the other hand, the reconstructed image will exhibit well-defined lobes, allowing a clear identification of the maxima and automatic skeletonizing using a simple peak detection algorithm.

This approach is somewhat similar to that of Schemm and Vest,[15] hence sharing some of its advantages; it uses the whole image, making it appropriate for interferograms exhibiting few fringes and deals with noise and nonuniform illumination. The advantage with respect to Schemm and Vest approach is the use of linear least squares fitting, providing a faster regularization and a method good enough to be implemented on dynamically changing interferograms, or even for the batch analysis of hundreds of them (for example, the results in the Appendix were obtained contaminating 1000 images of 401×405 pixels with noise and reconstructing them in less than 20 sec).

Our approach can also be compared with the representation by means of an array of Gaussians.[1] Even when this was intended to fit wavefront representation in the presence of sharp local deformations, the same idea can be used to smooth data and for maximum determination in the vicinity of a fringe maximum. In order to perform the fitting process, it is recommended to use an iterative process. The concept of Gaussian fitting is far more intuitively clear, but the computer implementation using standard linear least square fitting is easier using the approach presented here. As it has been largely studied for many years, least squares algorithms have been largely optimized and can be easily parallelized if necessary (the process itself can be parallelized, given that each slice operation is fully independent).

This procedure also exhibits one advantage in comparison with Fourier based spatial filtering:[6] edge effects are not as strong as in those methods. A few residual oscillations with very low amplitudes can be seen beyond the edges, but they are usually filtered in the binarization step of the skeletonizing.

In a future work, we will give a complete review on how to use the process for regularization, background suppression, band tracking, and feature extraction.

Appendix

This section address computing performance of the algorithm and quality reconstruction of the Bessel smoothing process against Wiener adaptive filter, which perform a similar regularization.

One of the advantages of our process is the speed of computation. Figure 8 shows a benchmark analysis performed over 10 generated shearograms of different sizes. The reported time corresponds only to the smoothing process using 100 Bessel functions with spatial frequency parameter $\alpha = 1$ and to the maxima detection. The inset shows the interferogram under analysis. The images are not always squared, given that the shearing parameter is normalized as a function of the side of the image, and being most noticeable as the size of the images increases. The computations were performed in a laptop using i7 Intel processor and 4 GB of RAM memory; the code was developed using MATLAB.

Even when the process was conceived as a regularization tool for unambiguously specify the center of an interference fringe, it has show itself as an image filter that can deal with noise. In order to investigate this feature further, we

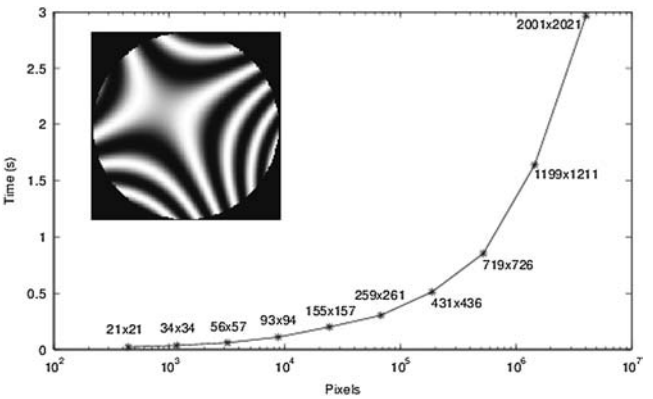

Fig. 8 Time spent performing smoothing of the interferogram for different values of total pixels. The specific image size is shown for each computational experiment. The inset shows the interferogram under consideration.

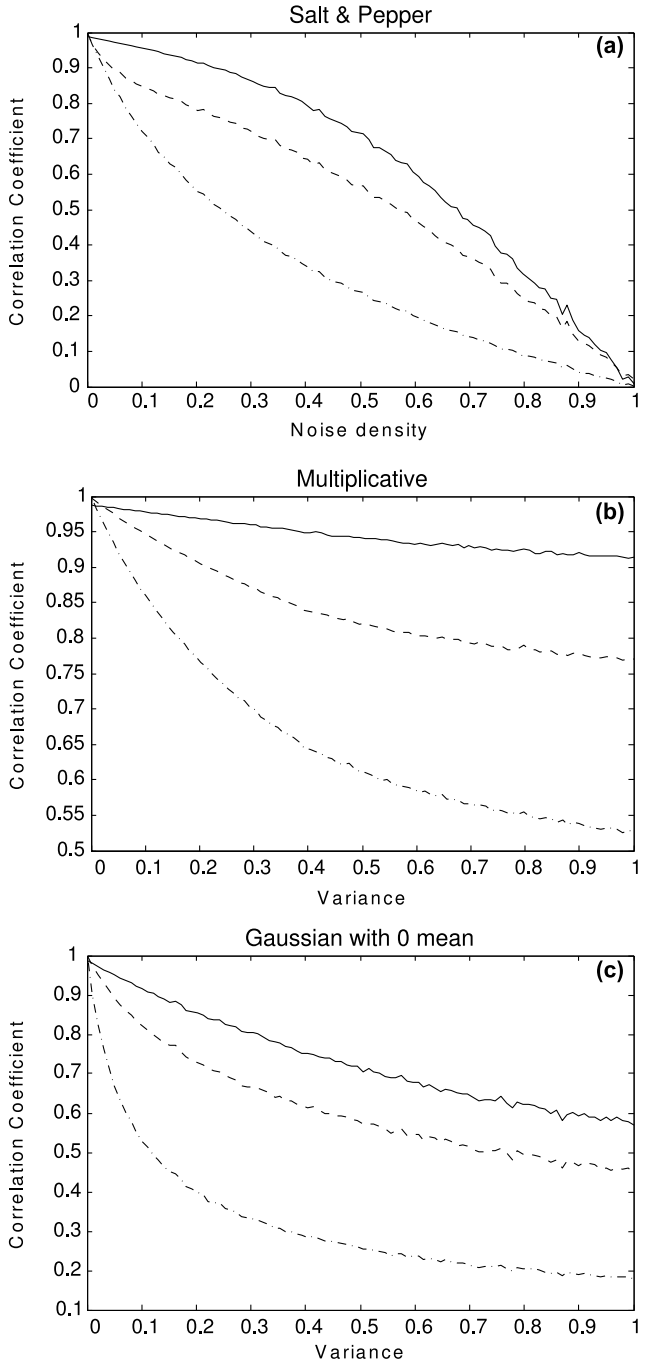

Fig. 9 Correlation coefficient as function of the characteristic parameter for each noise model. The dot-dashed line represents the correlation coefficient for the contaminated image with: (a) salt and pepper; (b) multiplicative noise; and (c) Gaussian with mean 0. The solid line represents the correlation coefficient for the reconstructed image using Bessel functions, the dashed line represents the correlation coefficient for the reconstructed image using Wiener adaptive filter.

have simulated six different shearograms with vertical, horizontal, circular bands, and a combination of these. We contaminated these shearograms with three different noises and reconstructed them using the Bessel functions and the Wiener[11] adaptive filter, which has been largely used for processing interferograms.[7] For characterizing the process, it was necessary to use a full-reference image quality assessment. We decided to use the image correlation coefficient:

$$r = \frac{\sum_m \sum_n (A_{mn} - \bar{A})(B_{mn} - \bar{B})}{\sqrt{\left[\sum_m \sum_n (A_{mn} - \bar{A})^2\right]\left[\sum_m \sum_n (B_{mn} - \bar{B})^2\right]}}, \quad (4)$$

where A and B are $M \times N$ matrices whose entries represent the intensity values sampled over some region and expressed in an arbitrary scale (in this case, normalized to 1). This quantity will evaluate to 1 when the images are exactly identical, and 0 when completely different. Our tests were carried out using impulse (salt and pepper), Gaussian, and multiplicative noises. We computed the correlation coefficient of both the contaminated and reconstructed images with respect to the original interferogram (Fig. 3). The process was repeated 25 times for each value of the characteristic parameter of the noise model, and averaged. The results can be seen on Fig. 9.

The Bessel smoothing process can greatly diminish the effects of the salt and pepper noise [Fig. 9(a)]. The image degradation (dot-dashed line) occurs following a concave curve, where the probability density represent the probability of each pixel switching to on (1) or off (0), while the degradation of the reconstructed image using both filters exhibits a convex behavior. The effect is most noticeable around the probability density 0.5. The Bessel smoothing (solid line) does better than the Wiener adaptive filter (dashed line).

The multiplicative noise used, Fig. 9(c), follows: $I = I_o + kI_0$, where k is a uniformly distributed random noise with mean 0 and variance v. This kind of noise slowly degrades the image, but still allowing to extract information from it. The Bessel functions reconstruction, however, works very well with this kind of noise and improves the image quality better for higher values of the variance. Bessel smoothing clearly outperforms the Wiener filter for this kind of noise.

On the other hand, the smoothing process and Wiener filter performs similarly on Gaussian noise [Fig. 9(b)]. We choose to use Gaussian white noise with 0 mean and variance ranging from 0 to 1. In this scenario, the process works the best for higher values of the variance.

Acknowledgments

The authors would like to thank Dr. Javier Sánchez-Mondragón and Dr. Gonzalo Urcid for interesting commentaries, and M.C. Alfonso Salas Sanchez for providing experimental information. This work is funded by CONACYT, Mexico. Romero-Antequera and Penalver would like to thank CONACYT for scholarships with numbers: 223982 and 23980, respectively.

References

1. D. Malacara, M. Servin, and Z. Malacara, *Interferogram Analysis for Optical Testing*, Taylor & Francis Group, Boca Raton, FL, 2nd ed. (2005).
2. T. Kreis, *Handbook of Holographic Interferometry*, WILEY-VCH GmbH and Co. KGaA, Weinheim (2005).
3. J. C. Wyant and C. L. Koliopoulos, An optical profilometer for surface characterization of magnetic media, *ASLE Trans.* **27**(2), 101–113 (1984).
4. M. Takeda, H. Ina, and S. Kobayashi, Fourier-transform method of fringe-pattern analysis for computer-based topography and interferometry, *J. Opt. Soc. Am* **72**(1), 156–160 (1982).
5. S. Gudmundsson, J. Michael Carstensen, and F. Sigmundsson, "Unwrapping ground displacement signals in satellite radar interferograms with aid of gps data and mrf regularization," *IEEE Trans. Geosci. Rem. Sens.* **40**(8), 1743–1754 (2002).

6. C. Roddier and F. Roddier, "Interferogram analysis using fourier transform techniques," *Appl. Opt.* **26**(9), 1668–1673 (1987).
7. C.-L. Tien, S.-S. Jyu, and H.-M. Yang, "A method for fringe normalization by zernike polynomial," *Opt. Rev.* **16**(2), 173–175 (2009).
8. J. H. Yi et al., "Peak movement detection method of an equally spaced fringe for precise position measurement," *Opt. Eng.* **41**(2), 428–434 (2002).
9. J. Rosenthal and D. S. Gilliam, *Mathematic Systems Theory in Biology, Communications, Computation*, Springer, Finance (2002).
10. A. Albert, *Regression and the Moore-Penrose Pseudoinverse*, Academic Press, Inc., New York, NY (1972).
11. J. S. Lim, *Two-Dimensional Signal and Image Processing*, Prentice Hall Inc., Englewood Cliffs, NJ (1990).
12. Y. Nativ, "Local maxima detection using image dilation," this code is publicly available at matlab central file exchange website, September 2007. http://www.mathworks.com/matlabcentral/fileexchange/14498-local-maxima-minima.
13. P. Senthilkumaran, J. Masajada, and S. Sato, "Interferometry with vortices," *Int. J. Opt.* **2012**(517591), 18 pages (2012).
14. T. Y. Kong and A. Rosenfeld, *Topological Algorithms for Digital Image Processing*, Elsevier Science B. V., The Netherlands (1996).
15. J. B. Schemm and C. M. Vest, "Fringe pattern recognition and interpolation using nonlinear regression analysis," *Appl. Opt.* **22**(18), 2850–2853 (1983).

Dayana H. Penalver is a member of SPIE, currently a PhD student in the National Institute for Astrophysics, Optics, and Electronics (INAOE is the acronym in Spanish) in Puebla, Mexico. She received a BSc degree in physics in 2006 from the Carabobo University in Venezuela, and a MSc in optical science in 2008 from INAOE. She has experience in optical testing in the laboratory and simulations for development of optical systems. She also worked in fit of multidimensional experimental data of power spectral density for validation and modification of the general theory of Harvey-Shack.

David L. Romero-Antequera received his BSc in physics at the University of Carabobo, Venezuela, in 2005. He got his MSc in optical science from the National Institute for Astrophysics, Optics, and Electronics (INAOE is the acronym in Spanish) in 2008. Currently he is a PhD student at INAOE. He has a background in programming, specifically in simulation of electromagnetic phenomena and nonlinear optimization problems. His last research interest are about photonic crystal, structured media, and phase unwrapping problems.

Fermín-Salomón Granados-Agustín is a researcher in the Optics Department of the National Institute of Astrophysics, Optics, and Electronics INAOE, México. He received his BS degree in physics from the National University of Mexico UNAM in 1993. He received his MS degree and PhD degree in optics, respectively, in 1995 and 1998, both from the INAOE. He is a national researcher for the National System of Researchers, Mexico. He held a postdoctoral position at the Mirror Lab of the Steward Observatory at the University of Arizona in 1999. He has been the head of the optical shop at the INAOE since 2005. His research interests include optical information, interferometric optical testing, and instrumentation.